J Electroceram (2009) 23:512–518
DOI 10.1007/s10832-008-9523-1

Effects of sputtering pressure and thickness on properties of ZnO:Al films deposited on polymer substrates

Jae-Hyeong Lee

Received: 29 May 2007 / Accepted: 5 May 2008 / Published online: 1 June 2008
© Springer Science + Business Media, LLC 2008

Abstract Highly conducting and transparent aluminum doped zinc oxide (ZnO:Al) thin films have been deposited on polyimide substrate by r.f. magnetron sputtering at room temperature. The influence of sputter pressure and thickness on the structural, electrical, and optical properties of ZnO:Al films deposited on polyimide substrate is reported. The crystallinity and degree of orientation was increased by decreasing the sputter pressure. For higher sputtering pressures an increase on the resistivity was observed due to a decrease on the mobility and the carrier concentration. As the film thickness was increased, the crystallite sizes were increased, but the average transmittance in the wavelength range of the visible spectrum was decreased. The electrical performances of the ZnO:Al films deposited on glass substrates are slightly worse than the ones of the films deposited on polyimide substrates with same thickness. The lowest resistivity of 8.6×10^{-4} Ω cm can be obtained for films deposited on glass substrate with the thickness of 800 nm.

Keywords Al-doped ZnO (ZnO:Al) · Sputtering · Polymer substrate · Sputter pressure, thickness · Solar cell

1 Introduction

Doped ZnO thin films are one of the most promising transparent conductive oxides to replace ITO in advanced applications such as displays, solar cells, optoelectronic devices, electrochromic devices [1–3] because of their material low cost, relatively low deposition temperature, non-toxicity and its stability in hydrogen plasma [4]. Recently, plastic materials are replacing glass substrates in a variety of applications due to its lower cost associated with its lighter weight. However, these substrates present certain challenges such as considerably lower working temperature and rougher surfaces as compared to glass substrates [5]. In order to overcome these limitations, r.f. magnetron sputtering process should be optimized to be able to produce highly transparent and highly conductive films exhibiting a low film stress and with a smooth surface. The characteristics of films are generally affected by preparation conditions, such as the deposition methods, working pressure, substrate temperature, types of substrates, and the thickness of films [6].

In this work, we present the effects of sputter pressure and thickness on the electro-optical properties of aluminum doped ZnO (ZnO:Al) films. ZnO:Al films were deposited on polyimide substrates by a r.f. magnetron sputtering. A parallel experiment onto a glass substrate was also carried out for comparison.

2 Experimental

The ZnO:Al films were deposited on Corning 7059 glass and polyimide substrates in a conventional r.f. magnetron sputtering system. The glass substrates were ultra-sonically cleaned in acetone and methyl alcohol, rinsed in deionized water, and subsequently dried in flowing nitrogen gas before deposition. The polymeric substrates only were ultrasonically cleaned in methyl alcohol. A sintered ceramic target with a mixture of ZnO (99.99% purity) and Al_2O_3 (99.999 purity) was employed as source materials. The

J.-H. Lee (✉)
School of Electronics and Information Engineering,
Kunsan National University,
San 68, Miryong-dong, Kunsan,
Jeollabuk-do, South Korea, 573-701
e-mail: jhyi@kunsan.ac.kr

amount of Al_2O_3 added to the target was 2.5 wt.%. The diameter of the target was 4 inch and target-to-substrates distance was 7 cm. A Turbo-molecular pump coupled with a rotary pump was used to achieve the pressure of 9.33×10^{-5} Pa before introducing argon gas. During deposition process, the sputter power was maintained at 125 Watt and the frequency is 13.56 MHz. The pressure of Ar was controlled from 0.27 to 2.7 Pa. The substrate temperature was measured using a thermocouple gauge and the substrate was kept at room temperature initially. At the film deposition, the substrate temperature was increased due to the bombardment of the sputtering ions and the final temperature was nearly 70°C. The ZnO:Al films with various thicknesses are obtained by varying the deposition time.

3 Results and discussion

The deposited films on the polyimide substrates were physically stable and present very good adherence to the substrates. No break or peel off of the films was observed when the films were folded many times or boiled for several hours in water.

Figure 1 shows the influence of sputtering pressure on the deposition rate of ZnO:Al films. The rate decrease at higher pressure is attributed to the increased number of collisions of sputtered molecules with gas molecules, leading to a thermalization of the film-forming particles [7]. Therefore, the diffusive ability of the atoms or molecules decreases, which results in the decrease of the deposition rate [8]. The lower deposition rate leads to layers with granular crystals separated by open, voided boundaries caused by the low energy of the sputtered species that contribute to the film growth [7], as can be confirmed by the SEM analysis (Fig. 3).

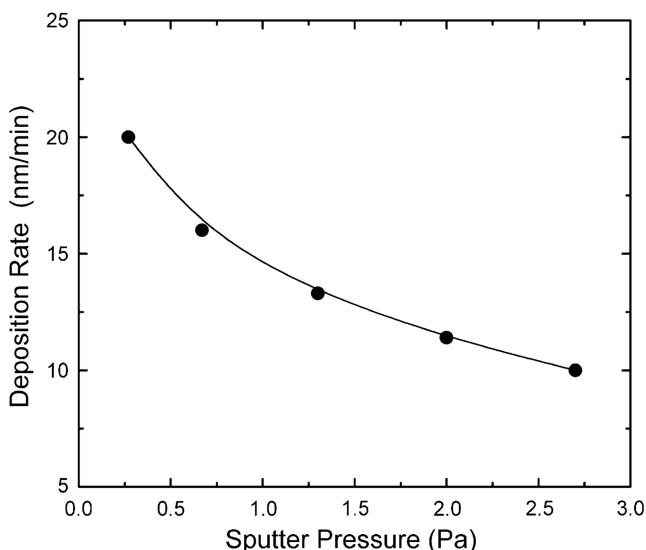

Fig. 1 Dependence of deposition rate of ZnO:Al films on the sputtering pressure. The substrate type is glass and the film thickness is about 400 nm

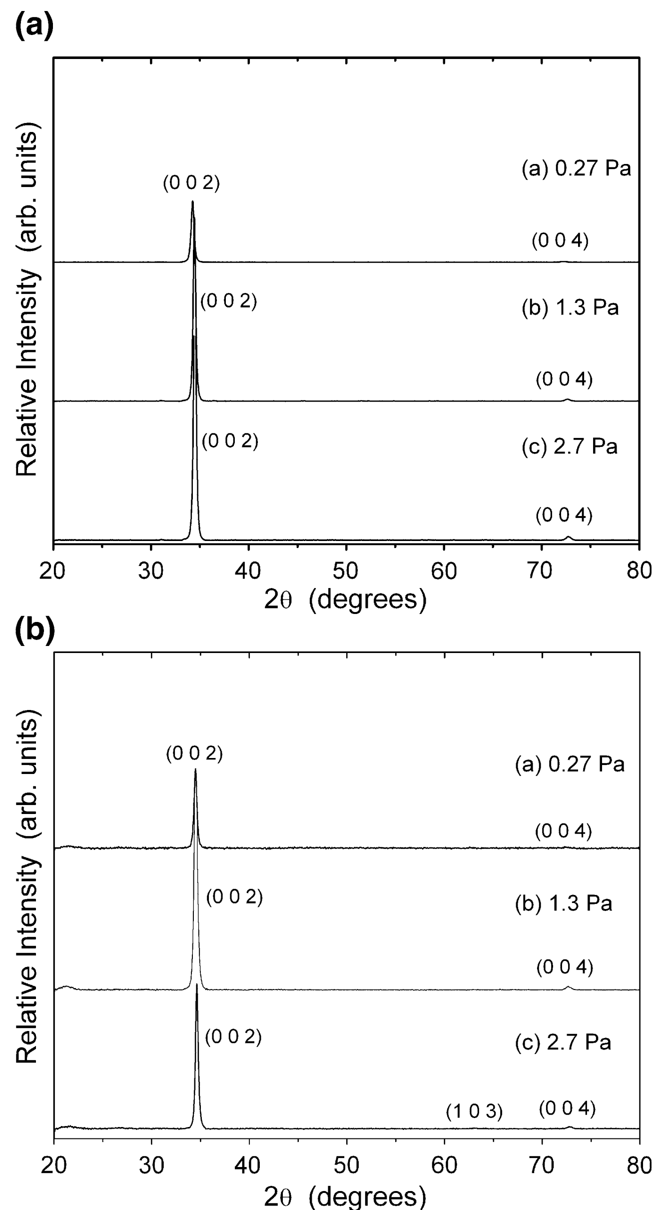

Fig. 2 XRD patterns for the ZnO:Al deposited at different sputter pressures: (**a**) glass substrate; (**b**) polyimide substrate. The thickness of all samples is about 400 nm

Figure 2 show the X-ray diffraction (XRD) patterns for the ZnO:Al deposited at different sputter pressures. The film on glass exhibit a strong peat at $2\theta=34.3°$ and a weak peak at $2\theta=72.3°$. These peaks are associated with the (0 0 2) and (0 0 4) plane of hexagonal phase. The spectrum reveals that all of the obtained films are polycrystalline with the hexagonal wurtzite structure and have a preferred orientation with the *c*-axis perpendicular to the substrates, regardless of sputter pressure and substrate types. Fujimura et al. [9] reported that sputtered ZnO thin films were

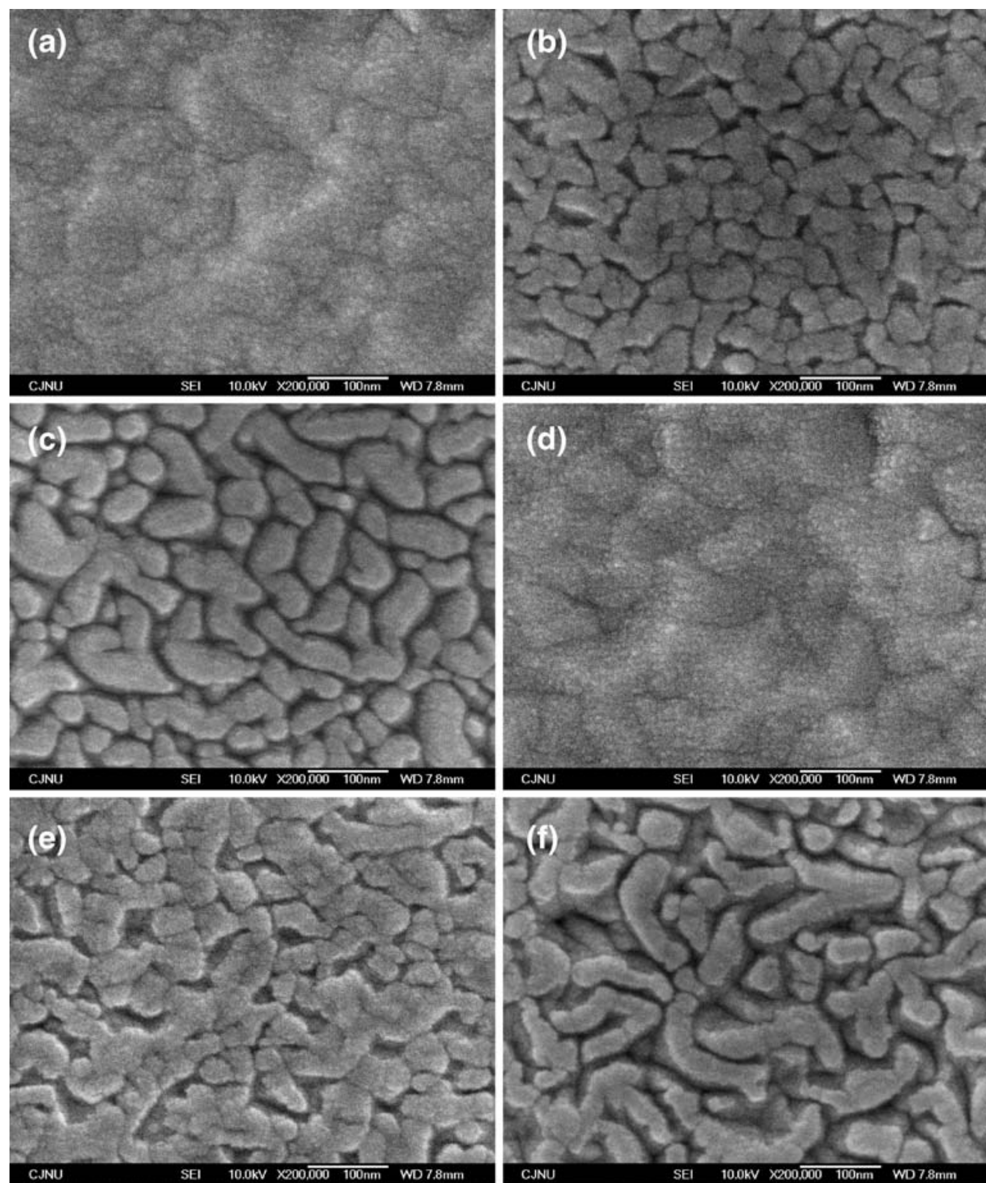

Fig. 3 SEM micrographs for ZnO:Al films deposited at different sputter pressures. Glass substrate: (**a**) 0.27 Pa, (**b**) 1.3 Pa, (**c**) 2.7 Pa; Polyimide substrate: (**d**) 0.27 Pa, (**e**) 1.3 Pa, (**f**) 2.7 Pa. The thickness of all samples is about 400 nm

generally polycrystalline with a *c*-axis preferential orientation due to the lowest surface free energy of (0 0 2) plane in ZnO. In the equilibrium state, the films grow with the plane of the lowest surface free energy parallel to the surface if there is no effect from the substrate [10]. Zinc oxide has tetrahedral coordination formed by the sp^3 hybridized orbit. When it has the wurtzite structure, the direction of each apex is parallel to the *c*-axis, [0 0 2]. This is why the ZnO films tend to grow toward the [0 0 2] direction [11]. The location of the (0 0 2) peaks does not shift significantly with decreasing sputter pressure, but the intensity become more intense and sharper. This is because the crystallinity of the films is improved and the crystallite size becomes larger with the sputter pressure. Song et al. [12] reported that the films deposited under high Ar pressure show diffraction peaks associated with (1 0 1) and (1 1 2) as well as (0 0 2) and (0 0 4). This result suggests that during the processing, some grains grow with other orientations for high Ar pressure. Neither metallic zinc or aluminum characteristic peaks nor aluminum oxide peak was observed from the XRD patterns, which implies that aluminum atoms replace zinc in the hexagonal lattice or aluminum segregate to the noncrystalline region in grain boundary [13]. In compared with the films deposited on the glass, the intensity of the diffraction peak for the films deposited on polyimide is somewhat weaker and the half-width is wider. This indicates that, under the same deposition conditions, the crystallite sizes of the films deposited on polyimide substrate are smaller than that deposited on glasses.

Figure 3 show the surface micrographs for ZnO:Al films deposited at different sputter pressures. It was found that the sputter pressure has a great influence on the surface

structure of the film. The morphology of ZnO:Al films deposited at lower pressure (<0.67 Pa) was found to be continuous and dense with the grain size of 100 nm. Danson et al. concluded that the lower argon pressure gave the higher coating quality and the efficient sputtering system [14]. At higher pressure (>1.3 Pa), the surface consists of elongated crystallites separated by voids, regardless of substrate type. In this pressure region, the grain size of the films becomes larger with decreasing sputter pressure.

The electrical properties of the ZnO:Al films as a function of sputter pressure is show in Fig. 4. It is observed that the resistivity of the films is increased with increasing the sputter pressure. A similar behavior was observed by Assuncao et al. [7]. At high pressure the sputtered species undergo many collisions leading to a thermalization of the film-forming particles. Therefore, the energy of the ions become smaller and the bonding energy become weaker that caused

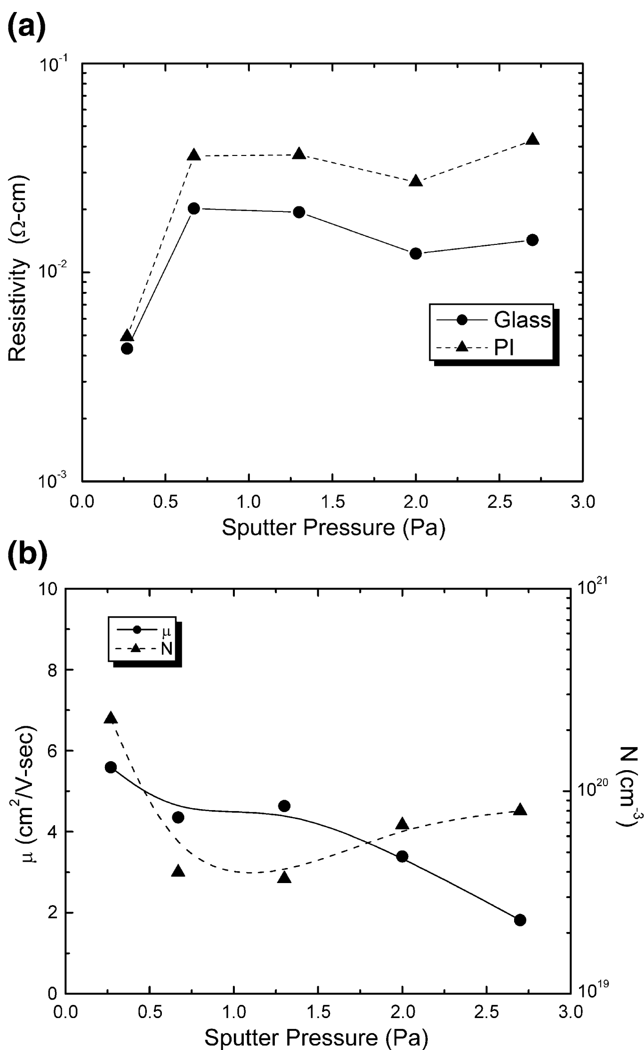

Fig. 4 Influence of sputter pressure on the electrical properties of ZnO:Al films: (**a**) electrical resistivity, (**b**) Hall mobility and carrier concentration of ZnO:Al films deposited on polyimide substrate. The thickness of all samples is about 400 nm

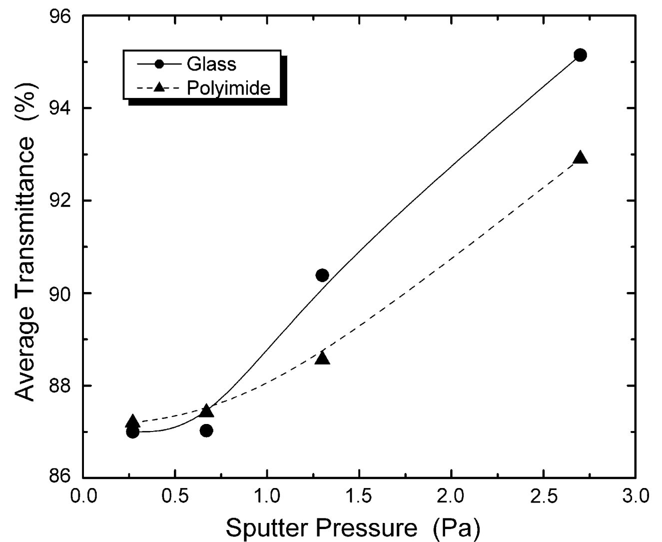

Fig. 5 Average transmittance in the range of 450~850 nm for the ZnO:Al films deposited at different pressures. The thickness of all samples is about 400 nm

the crystallinity of the films get bad. However, if the pressure is too low, the system is difficult to discharge or the plasma is unstable. In addition, the Hall mobility (μ) and the carrier concentration (N) are reduced when the films are deposited at higher pressure. The decrease in mobility may be due to the increased grain boundary scattering [15] as the size of the crystallites are likely to be smaller at a high working pressure during deposition. This would be happen because the sputtered neutrals arrive at the substrate with less kinetic energy due to increased scattering and hence have less energy for migration along the substrate surface.

Figure 5 shows the average transmittance in the range of 450~850 nm for the ZnO:Al films deposited at different pressures. The average transmittance over 90% is detected in the visible spectrum range for films deposited above 2 Pa, but the average transmission drops slightly to 87% below 1.0 Pa. The improvement of optical transmittance at higher pressure is caused by voids in films as seen in SEM results (Fig. 3).

X-ray diffraction (XRD) patterns of the ZnO:Al films on the glass and the polyimide substrates with different thicknesses are shown in Fig. 6. All the films were deposited at 125 W and 0.27 Pa. They reveal that all films are polycrystalline and retain the hexagonal structure. The films exhibit one strong peak at $2\theta{\sim}34.3°$ related to (0 0 2) plane of the hexagonal phase and two weak peak at $2\theta{\sim}62.5°$ and 72.4° related to (1 03) and (0 0 4) planes. This indicates that these films have a (0 0 2) preferred orientation. According to the kinetics of crystal growth [16–18], the growing faces of a crystal are part of the free surface of the film. These crystal faces correspond to the crystal shape at equilibrium and are determined by the orientation of the crystal. A growth competition can start

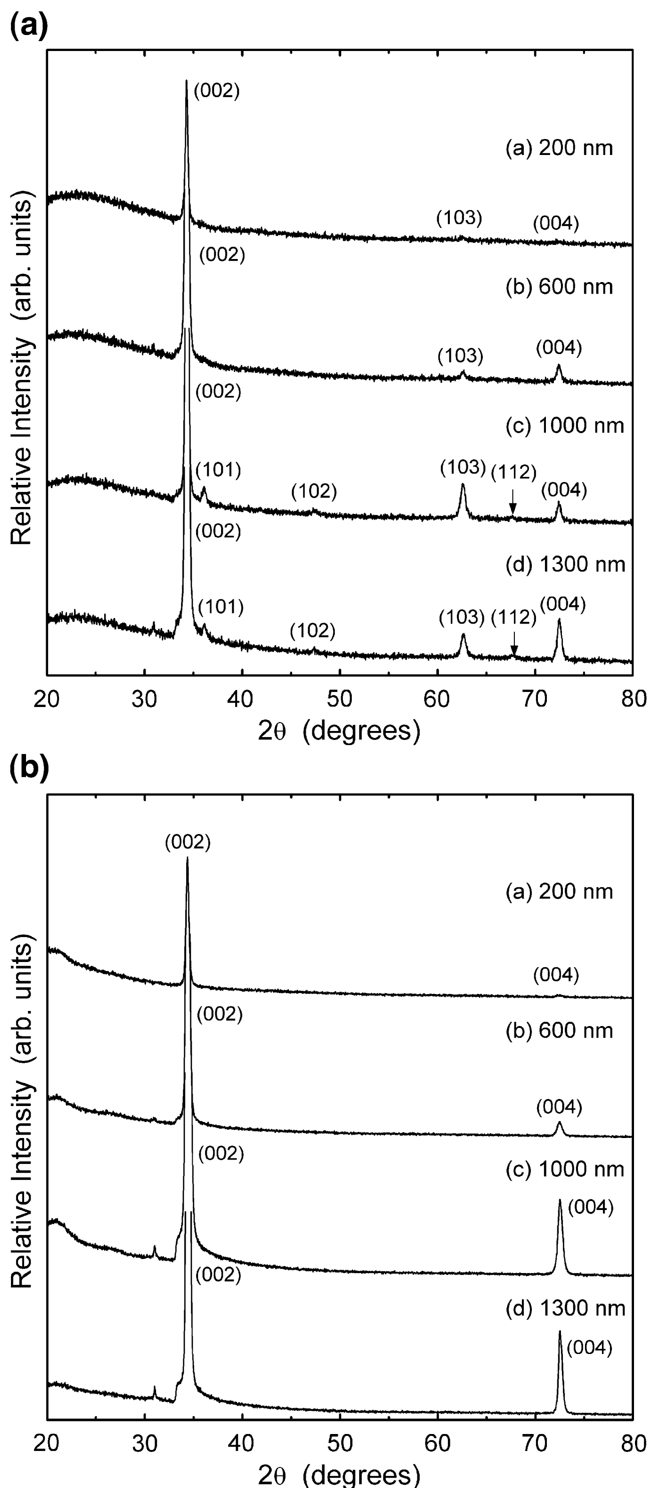

Fig. 6 XRD patterns of the ZnO:Al films with various thicknesses on (**a**) glass substrate (**b**) polyimide substrate

among the neighboring crystals according to their growth types (i.e., to their orientation). The faster growing crystals will grow over the slower growing ones. This competition is terminated when only crystals exhibiting the same type of crystal faces proceed to the free surface. This competitive crystal growth represents an orientation selection among the crystals resulting in the competitive growth texture [19]. As the thickness increases, the location of the peaks does not change significantly, but the intensity of these peaks becomes more intense and shaper, suggesting that the grain size of the films becomes larger with increasing the film thickness. This was probably why the crystallinity was increased when the ZnO:Al film was thicker. In addition, for the films thicker than 1 μm, new diffraction peaks are shown at 2θ~36.1°, 47.4°, and 67.7°, which is associated with the (1 0 1), (1 0 2), and (1 1 2) plane of the hexagonal phase. For comparison purposes the XRD pattern of the polyimide substrate also shows in Fig. 5(b). As the thickness increases the diffraction peaks become sharper and larger (as expected) while those locations do not change significantly. This behavior means that no significant residual stresses are generated during the deposition process and that the crystallite size is increased with the film thickness.

Figure 7 show the variation of full width at half maximum (FWHM) of (0 0 2) peak and crystallite size of ZnO:Al films deposited on polyimide substrate as a function of film thickness. The crystallite sizes of films were calculated by using Scherrer's formula [20, 21]. As the thickness increases from 200 nm to 1.3 μm, the FWHM decreases from 0.25° to 0.12° and the crystallite size enlarge.

From the SEM analysis, the crystallite size of ZnO:Al films enlarged with increasing the film thickness. When the deposition begins, there are many nucleation centers on the substrate and small crystallites are produced. The films are deposited for only a short time, the small crystallites on the substrate are not able to grow into large crystallites, and therefore the thinner films have smaller crystallites than the thicker films. With increasing film thickness, the crystallinity of the films is improved and the crystallite sizes become larger. These are consistent with the XRD results.

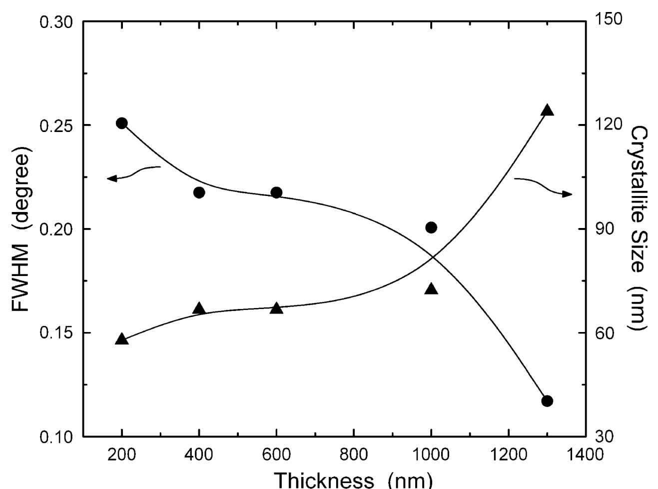

Fig. 7 FWHM of (0 0 2) peaks and crystallite size of ZnO:Al films deposited on polyimide substrate as a function of thickness

In addition, it is possible to observe the cross sectional view of the film, where a high compact and dense columnar structure is clearly seen.

Figure 8 shows the electrical resistivity of the ZnO:Al films deposited on the glass and the polyimide substrates as a function of thickness. The resistivity of films is reduced with increasing film thickness, regardless of substrate types. As seen in XRD and SEM results, the enhancement of the conductivity is attributed to the improvement of the crystallinity and the larger grain sizes. The resistivity of thicker film and very thin films could be expressed by Eqs. (1) and (2), respectively [22].

$$\frac{\rho_f}{\rho_0} = 1 + \frac{3}{8K} \quad (K >> 1) \tag{1}$$

$$\frac{\rho_f}{\rho_0} = \frac{4}{3K \ln \frac{1}{K}} \quad (K << 1) \tag{2}$$

Here ρ_f is the resistivity of thin film, ρ_0 is the resistivity of bulk, and K is the reduced thickness (K=the film thickness/ the mean free path of the charge carrier in the bulk material). From Eqs. (1) and (2), it can be seen that the influence of film thickness on the resistivity becomes smaller for thicker films. In addition, the resistivity is decreased with increasing the film thickness. The resistivity of ZnO:Al films in this study had a similar behavior. The films with the thickness of 800 nm exhibit the lowest resistivity (8.6×10^{-4} Ω cm for glass substrate and 9.5×10^{-4} Ω cm for polyimide substrate). As the thickness increases further, the resistivity for the ZnO:Al films slightly increases, regardless of substrate types.

Figure 9 shows the Hall mobility and the free carrier concentration of ZnO:Al films with various thicknesses. The Hall mobility is increased with increasing the film

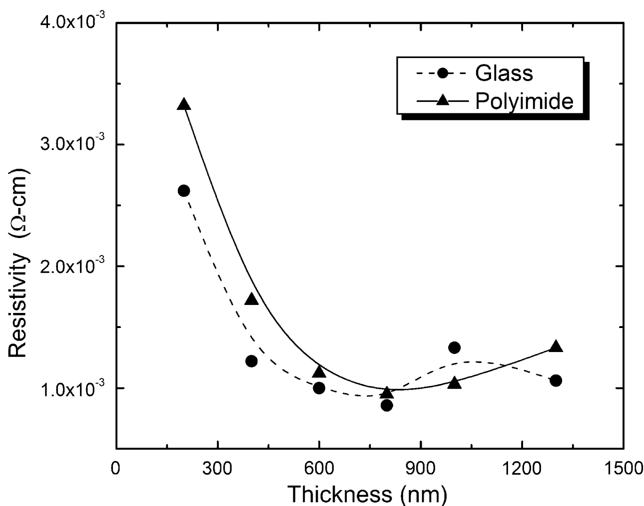

Fig. 8 Dependence of electrical resistivity on the ZnO:Al film thickness

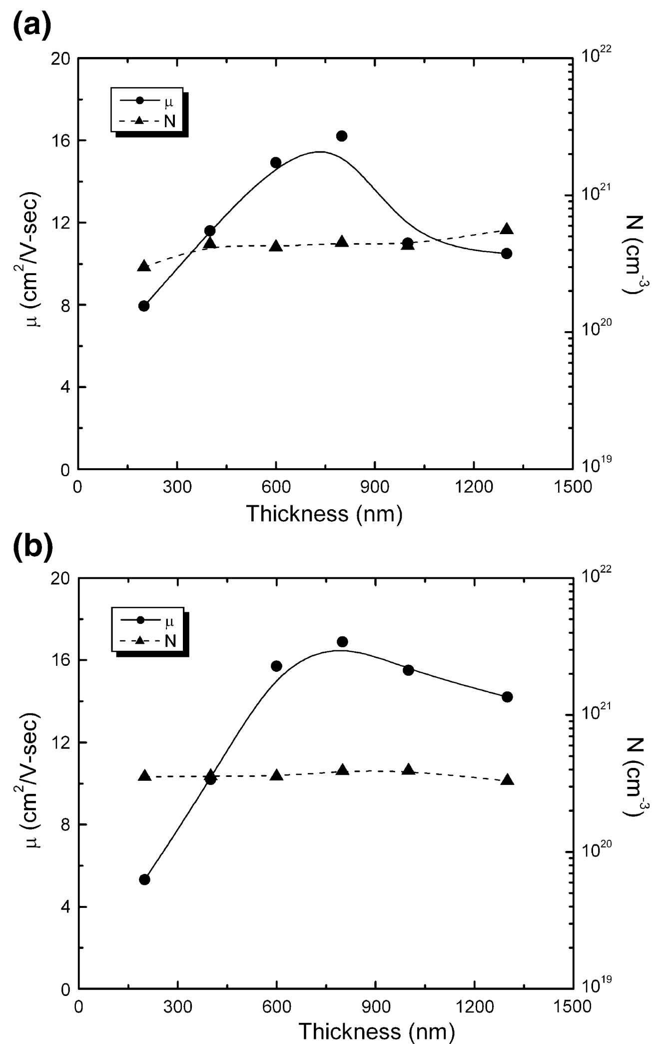

Fig. 9 Carrier concentration (*N*) and Hall mobility (*m*) as a function of film thickness: (**a**) glass substrate, (**b**) polyimide substrate

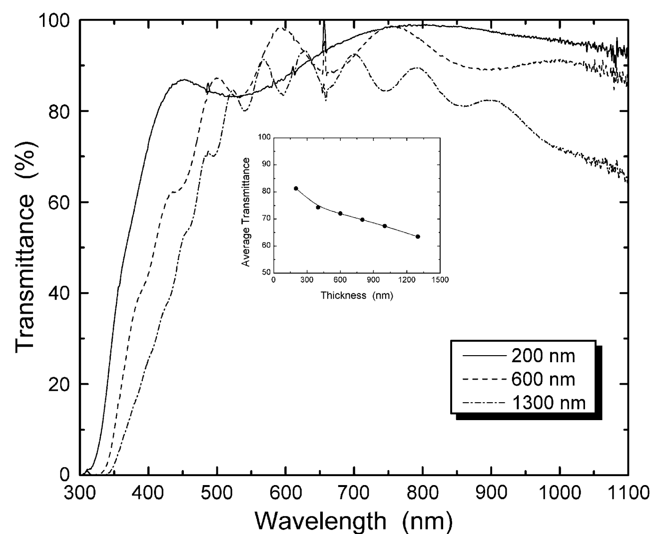

Fig. 10 Optical transmittance of ZnO:Al films deposited on the glass substrate with various thicknesses. The values of optical transmittance were modified by using that of blank glass substrate. An inserted graph is the average transmittance in the range of 300~800 nm

thickness while the carrier concentration is increased slightly (for the glass substrate) or constant (for the polyimide substrate). The increased mobility for the thinner films is attributed to the enhancement of the crystallinity and the enlargement of the grain that weakens inter-crystallite boundary scattering and increases carrier lifetime [23]. The resistivity is proportional to the reciprocal of the product of carrier concentration (N) and mobility (μ) as the following equation:

$$\rho = \frac{1}{qN\mu} \tag{3}$$

As seen in Fig. 8, the ZnO:Al film with the thickness of 800 nm had the lowest resistivity, which resulted from the lowest product of the carrier concentration and the mobility. When the ZnO:Al films were thick enough, however, the mobility is reduced, regardless of substrate types. The film with the thickness of 1.3 μm has very rough surface due to large grains. The surface roughness could generally affect the carrier mobility [24]. Therefore, the reduction in mobility is attributed to the rough surface of ZnO:Al films.

Figure 10 shows the optical transmittance in the range of 300~1,100 nm for ZnO:Al films deposited on the glass substrate with various thicknesses. For transmittance measurement, the beam was made to enter the film and a blank glass substrate was kept in the path of the reference beam for compensation. With increasing the thickness, the transmittance of the films is reduced due to thickness effect. The average transmittance in the range of 300~800 nm is decreased from 81.2% to 63.5% when the film become thicker from 200 nm to 1,300 nm. As the thickness of the ZnO:Al films is increased, the near-infrared transmittance decrease. In addition, the absorption edge was observed at a longer wavelength range for thicker ZnO:Al film. The shift of absorption edge may be attributed to the difference in grain size [25]. As shown in XRD and SEM results, the thinner ZnO:Al film contained relatively small grain size, this was probably why the blue shift occurred. As the thickness of the ZnO:Al films is increased, the optical band gap, which is calculated by extrapolating the $(\alpha h\nu)^2$ values to $h\nu$=0 from $(\alpha h\nu)^2$ versus $h\nu$ plots, is decreased from 3.64 eV to 3.51 eV. These values are larger than that for pure ZnO (~3.3 eV) because of Burstein–Moss shift [26]. The films deposited on the polyimide substrates exhibit the similar trend.

4 Conclusions

ZnO:Al thin films were deposited on polyimide and glass substrate by r.f. magnetron sputtering. The structural, electrical, and optical properties of the films depended on the sputtering pressure and the thickness. The ZnO:Al films were polycrystalline and retained the hexagonal structure with the (0 0 2) preferred orientation, regardless of sputter pressure and thickness. As the sputter pressure increased, the grain size of films became larger and the optical properties were improved. However, the conductivity of the films was deteriorated with increasing the sputter pressure. With increasing the film thickness, the crystallite sizes and the conductivity were enhanced. The lowest resistivity of 8.6×10^{-4} Ω cm can be obtained for films deposited on glass substrate with the thickness of 800 nm. The average transmittance of the film with 200 nm thickness was over 80% and it was reduced with increasing film thickness. These results fulfill the minimum requirements necessary for producing transparent electrodes on flexible optoelectronic devices using polymeric substrates.

Acknowledgement This work has been supported by KESRI (R-2005-7-147), which is funded by MOCIE (Ministry of Commerce, Industry and Energy).

References

1. K. Vanheusden, W.L. Warren, C.H. Seager, J. Appl. Phys. **79**, 7983 (1996)
2. K.L. Chopra, S. Major, Thin Solid Films **102**, 1 (1983)
3. C.G. Granqvist, Thin Solid Films **193–194**, 730 (1990)
4. D. Song, A.G. Aberle, J. Xia, Appl. Surf. Sci. **195**, 291 (2002)
5. E. Fortunato, A. Gonçalves, V. Assunção, A. Marques, H. Águas, L. Pereira, I. Ferreira, R. Martins, Thin Solid Films **442**, 121 (2003)
6. W.T. Lim, C.H. Lee, Thin Solid Films, **353**, 12 (1999)
7. V. Assuncao, E. Fortunato, A. Marques, H. Aguas, I. Ferreira, M.E.V. Costa, R. Martins, Thin Solid Films **427**, 401 (2003)
8. K. Ellmer, J. Phys. D: Appl. Phys. **33**, R17 (2000)
9. N. Fujimura, T. Nishihara, S. Goto, J. Xu, T. Ito, J. Cryst. Growth **130**, 269 (1993)
10. W.K. Burton, N. Carberra, F.C. Frank, Philos. Trans. R. Soc. Lond. A **243**, 299 (1951)
11. S.-S. Lin, J.-L. Huang, Surf. Coat. Technol. **185**, 222 (2004)
12. D. Song, A.G. Aberle, J. Xia, Appl. Surf. Sci. **195**, 291 (2002)
13. X. Hao, J. Ma, D. Zhang, T. Yang, H. Ma, Y. Yang, C. Cheng, J. Huang, Appl. Surf. Sci. **183**, 137 (2001)
14. N. Danson, I. Safi, G.W. Hall, R.P. Howson, Surf. Coat. Technol. **99**, 147 (1998)
15. E. Shanti, A. Banerjee, V. Dutta, K.L. Chopra, J. Appl. Phys. **53**, 1615 (1982)
16. A. van der Drift, Philips Res. Rep. **22**, 267 (1967)
17. G. Knuyt, C. Quaeyhaegens, J. D'Haen, L.M. Stals, Thin Solid Films **258**, 159 (1995)
18. G. Knuyt, C. Quaeyhaegens, J. D'Haen, L.M. Stals, Phys. Status Solidi, B Basic Res. **195**, 179 (1996)
19. P.B. Barna, M. Adamik, Thin Solid Films **317**, 27 (1998)
20. L. Sagalowicz, G.R. Fox, J. Mater. Res. **14**, 1876 (1999)
21. G. Sanon, R. Rup, A. Mansingh, Thin Solid Films **190**, 287 (1990)
22. S.-S. Lin, J.-L. Huang, D.-F. Lii, Surf. Coat. Tech. **190**, 372 (2005)
23. X. Yu, J. Ma, F. Ji, Y. Wang, C. Cheng, H. Ma, Appl. Surf. Sci. **245**, 310 (2005)
24. T. Schuler, M.A. Aegerter, Thin Solid Films **351**, 125 (1999)
25. J. Yu, X. Zhao, Q. Zhao, Thin Solid Films **379**, 7 (2000)
26. E. Burstein, Phys. Rev. **93**, 632 (1954)